ISBN: 978-3-95450-132-8 doi:10.18429/JACoW-IPAC2014-TUPRO116

# CONCEPTUAL DESIGN OF THE MUON COOLING CHANNEL TO INCORPORATE RF CAVITIES*

S.A. Kahn#, G. Flanagan, F. Marhauser, Muons, Inc., Batavia, IL 60510, USA
M.L. Lopes, K. Yonehara, FNAL, Batavia, IL 60510, USA

*Abstract*

A helical cooling channel (HCC) consisting of a pressurized hydrogen gas absorber imbedded in a magnetic channel that provides solenoid, helical dipole and helical quadrupole fields has been shown to provide six-dimensional phase space reduction for muon beams. Such a channel can be implemented by helical solenoid (HS) channel composed of short solenoid coils arranged in helical pattern. The magnetic channel will provide the desired $B_\varphi$, $B_z$, and $dB_\varphi/dr$ along the reference path. The channel must allow enough space for RF cavities which replace the energy lost in the absorber material present for the cooling process. This study will describe how to achieve the desired field while allowing sufficient space for the cavities. The limits to this design imposed by the achievable current density in the coils will be discussed.

## INTRODUCTION

A high energy muon collider would be a unique energy frontier machine for the 21st century. Significant cooling of the muon beams would be necessary to obtain the high luminosity required to obtain the proposed physics program. A reduction of muon phase space by a factor of at least $10^6$ is required to achieve the necessary luminosity. Simulations have shown that the HCC can provide a significant phase space reduction [1] by ionization cooling. The HCC is composed of a magnetic channel filled with pressurized $H_2$ gas absorber to reduce the particle momentum in all dimensions. The lost energy is replaced in the longitudinal direction by RF. The desired field to hold the beam in a helical path in the magnetic channel is composed of helical dipole, helical quadrupole and solenoid components [2]. The helical dipole and quadrupole terms are given by the analytic expressions:

*Helical Dipole:*

$$B_\varphi = 2b_d I_1(k\rho)\frac{\cos(\varphi - kz)}{k\rho}$$
$$B_\rho = 2b_d I'_1(k\rho)\sin(\varphi - kz)$$
$$B_z = -k\rho B_\varphi$$

*Helical Quadrupole:*

$$B_\varphi = \frac{2b_q}{k^2\rho} I_2(2k\rho)\cos 2(\varphi - kz - \varphi_2)$$
$$B_\rho = \frac{2}{k} I'_2(2k\rho)\sin 2(\varphi - kz - \varphi_2)$$
$$B_z = -k\rho B b_\varphi$$

where $b_d$ and $b_q$ are the dipole and quadrupole strengths, respectively, at $\rho = 0$. Implementing this channel with helical harmonic coils is difficult since $I_n(nk\rho)$ grows exponentially at large radius and the channel has large apertures. The HCC magnetic channel can be implemented with short solenoid coils arranged along the helical reference orbit as is shown in Fig. 1 [3-4]. This approach minimizes the coil aperture which reduces the field on the coils. Fig. 1 shows the HS embedded in an external solenoid field (referred to as anti-solenoid). This allows $B_\varphi$ and $B_z$ to be set independently by adjusting the current to the HS and external anti-solenoid. $dB_\varphi/dr$ is important to control the beam focusing in the channel. To set field gradient to an arbitrary value requires an additional degree of freedom. A more complete description of achieving the desired helical solenoid fields is described elsewhere [5-7]. This paper will explore techniques to adjust the field gradient for the current HCC design.

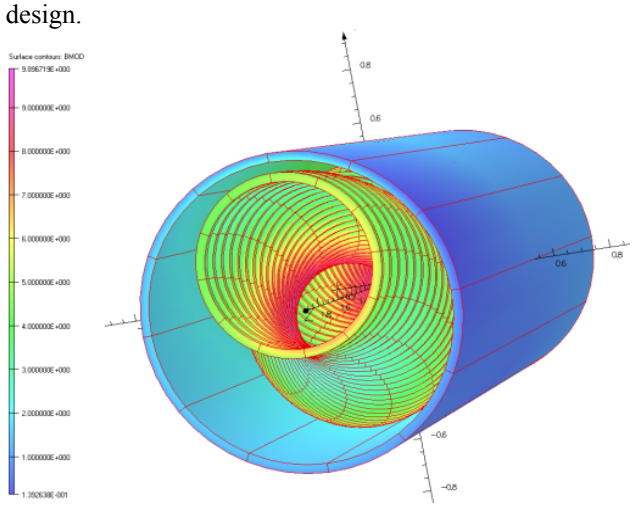

Figure 1: 3D layout of coils for the HCC channel. Note that the HS coils are placed in an external solenoid field. This sketch is from Ref [3].

## HCC CHANNEL DESIGN

The HCC is divided into several sections with each section providing a smaller final equilibrium emittance by using progressively shorter helical periods and larger fields. Table 1 shows the design field on the reference orbit for each section [8]. The field values are chosen to provide equal cooling in both transverse and longitudinal modes. The HS coils will need to be optimized to produce these fields.

*Work supported by U.S. DOE STTR/SBIR grant DE-SC00006266.
#kahn@muonsinc.com

ISBN: 978-3-95450-132-8 doi:10.18429/JACoW-IPAC2014-TUPRO116



Table 1: Field Properties of the HCC Sections

| Sect | f | λ | $B_\varphi$ | $dB_\varphi/dr$ | $B_z$ |
|---|---|---|---|---|---|
| Units | MHz | m | T | T/m | T |
| 1 | 325 | 1.0 | 1.29 | -0.50 | -4.25 |
| 2 | 325 | 0.9 | 1.43 | -0.62 | -4.73 |
| 3 | 325 | 0.8 | 1.61 | -0.79 | -5.32 |
| 4 | 650 | 0.5 | 2.58 | -2.01 | -8.51 |
| 5 | 650 | 0.4 | 3.22 | -3.14 | -10.63 |
| 6 | 650 | 0.3 | 4.30 | -5.58 | -14.18 |

There are design constraints imposed on the channel to accommodate the RF cavities. The inner radius of the coils must be large enough to allow space for the cavity, thermal isolation and coil support. Table 2 shows parameters describing the dielectric filled cavities that are being considered for the HCC [9-10]. The number of coils per period should be the same as the number of cavities per period. More coils-per-period produces better field quality. However increasing the number of cavities increases the cavity peak power losses. We have settled on 10-13 cavities per period as a compromise.

Table 2: Geometric Parameters of the RF Cavities

| Section | Frequency MHz | Cavities Per Period | Radius mm | Length mm |
|---|---|---|---|---|
| 1 | 325 | 13 | 280.2 | 77.3 |
| 2 | 325 | 13 | 280.2 | 69.0 |
| 3 | 325 | 13 | 280.2 | 60.7 |
| 4 | 650 | 13 | 140.1 | 35.7 |
| 5 | 650 | 13 | 140.1 | 27.3 |

## OPTIMIZING THE FIELD

$B_\varphi$ and $B_z$ can be set to the desired values by adjusting the currents in the HCC coils and the global anti-solenoid. There are limits to the size of anti-solenoid field because of cost considerations. We would like to restrict the anti-solenoid field to be small enough so that it could be wound with NbTi conductor. The field derivative, $dB_\varphi/dr$ which controls the focusing is more difficult to control. There are several approaches which affect $dB_\varphi/dr$:

- Placing the reference orbit and cavities away from the coil center will generate field gradient. However, this will lead to larger coils which would have larger fields on those coils, which we like to avoid.
- Deforming the coil into an elliptical shape. This has a significant effect on $dB_\varphi/dr$ and can be used to achieve the desired gradient [11].
- Tilting the coils. Not only does this have a beneficial effect on $dB_\varphi/dr$, it also produces helical dipole field.

### *Tilting the Coils*

Tilting the HCC coils will generate $B_\varphi$ proportional to the tangent of the tilt angle. Since this is added to the helical dipole from the HCC arrangement of coils, the current in the coils can be reduced. Reducing the current in the HS coils also reduces the $B_z$ produced by these coils. This reduces the anti-solenoid field required into the range attainable by NbTi conductor (as seen in Table 4). Figure 2 shows an arrangement of tilted HS coils. To provide room to tilt the coils the coil fill fraction is chosen to be 50%. This allows space to tilt the up to 200 to 250 mr. Also it allows extra space free on the opposite side for RF services, etc.

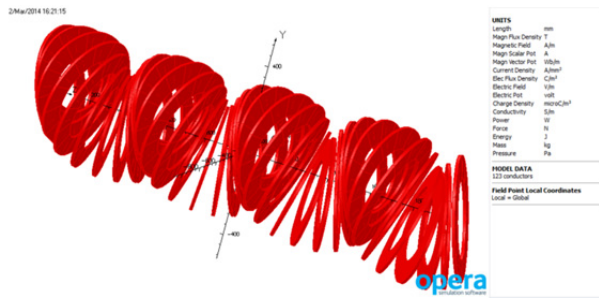


Figure 2: Configuration of HS coils for section 4 showing the tilted coils.

### *Elliptical Coils*

Deforming the coils into an elliptical shape also affects the $dB_\varphi/dr$ [11]. Fig. 3 shows $B_\phi$ as a function of radial position for section 5. Curves are plotted for different $A = \frac{(R_{major}-R_{minor})}{(R_{major}+R_{minor})}$. These curves display different slopes at the reference orbit position (where the curves cross).

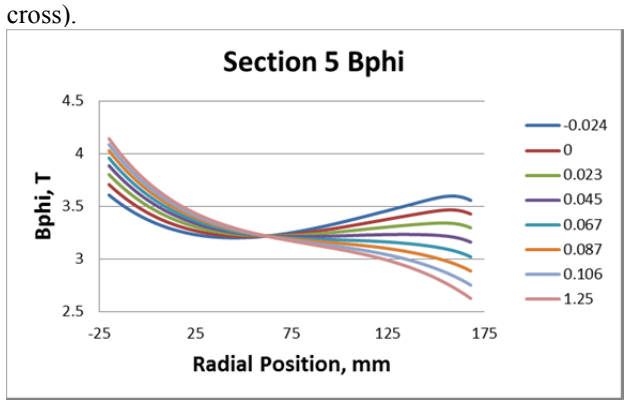


Figure 3: $B_\phi$ vs. r for section 5. The different colors represent different ellipse asymmetries.

Using both the tilted coil and the elliptical coil configurations the optimum solution is found for each section. Table 3 shows the geometries for the selected solutions for each section. *R_az* and *R_rad* are the azimuthal and radial coil inner radii and *dR* is the radial thickness of the coil. The fields associated with these cases are shown in Table 4. To reduce the coil sizes for section 5, it was necessary to use 975 MHz cavities.

ISBN: 978-3-95450-132-8 doi:10.18429/JACoW-IPAC2014-TUPRO116

Table 3: Coil Geometries of Selected Solutions

| Sect. | Period | R_az | R_rad | dR | Freq | Tilt |
|---|---|---|---|---|---|---|
| | m | mm | mm | mm | MHz | mr |
| **1** | 1.0 | 315 | 315 | 50 | 325 | 200 |
| **2** | 0.9 | 370 | 315 | 50 | 325 | 200 |
| **3** | 0.8 | 350 | 275 | 100 | 325 | 250 |
| **4** | 0.5 | 225 | 150 | 100 | 650 | 200 |
| **5** | 0.4 | 130 | 110 | 100 | 975 | 200 |

Table 4: Fields Associated with Selected Solutions

| Section | $J_E$ | $B_\phi$ | dB/dr | Anti-solenoid | Peak Field |
|---|---|---|---|---|---|
| | A/mm$^2$ | T | T/m | T | T |
| **1** | 216 | 1.289 | -0.609 | -1.13 | 9.24 |
| **2** | 289 | 1.432 | -0.651 | -2.7 | 11.78 |
| **3** | 304 | 1.611 | -0.677 | -3.66 | 13.09 |
| **4** | 320 | 2.479 | -2.135 | -6.08 | 16.79 |
| **5** | 347 | 3.220 | -3.129 | -7.33 | 19.56 |

## FIELD AT THE COIL

The limit of reached when the field at the coil limits the current that the conductor can carry. Figure 4 shows the field distribution on a single coil in the HCC from all the coils in the channel for section 4. The field peaks at the inner surface of the coil on the side closest to the helix axis where coil apertures overlap. Column 6 in table 4 shows the peak field on the coil for the different sections. For section 4 the current density is 50% of the critical current density for $Nb_3Sn$. Section 5 is above the limit for $Nb_3Sn$. It is still possible to use Bi-2212 for section 5. To reduce the field on the coil for section 5 will require modifying the cooling scheme itself. By favoring the longitudinal cooling decrement over the equal cooling decrement one could reduce the required field gradient which would also reduce the required coil current. This is being investigated.

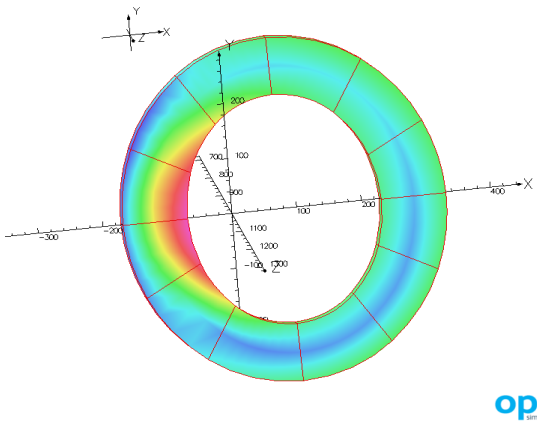


Figure 4: |B| on a coil is shown for section 4. The high field region is on the side of the coil closest to the helix axis.

## COIL FORCES

The forces between an individual coil and the HCC coil lattice can be calculated for configurations with different coil tilts. Table 5 shows the integrated radial force, $F_x$, and torque, $\tau_x$ on a coil oriented in the x direction from the other coils in the HCC. $F_y$, $F_z$, $\tau_y$ and $\tau_z$ are zero by symmetry in a long channel. Tilting the coils increases the horizontal force on the coil, however these forces can be supported by a stainless steel structure.

Table 5: Integrated Forces and Torques on a Coil from the HCC Channel

| Section | Tilt Angle | $F_x$ | $\tau_x$ |
|---|---|---|---|
| Units | mr | newtons | N-m |
| 3 | 0 | $-2.05\times10^6$ | $2.57\times10^5$ |
| 3 | 200 | $-3.18\times10^6$ | $-3.83\times10^4$ |
| 3 | 250 | $-2.88\times10^6$ | $-1.12\times10^5$ |
| 3 | 300 | $-2.67\times10^6$ | $-1.72\times10^5$ |
| 4 | 0 | $-1.46\times10^6$ | $8.10\times10^4$ |
| 4 | 200 | $-1.65\times10^6$ | $-1.57\times10^4$ |
| 4 | 300 | $-1.83\times10^6$ | $-6.64\times10^4$ |

## CONCLUSION

This report is to be considered preliminary as it is a work in progress. A magnet system is being designed for the HCC allowing for the larger aperture necessary for including RF cavities. In order to achieve the desired magnetic field and field gradient, it was necessary to tilt the coils and to deform the coils into an elliptical shape. This approach provides a possible solution for a magnet system with RF cavities.

## REFERENCES

[1] K. Yonehara et al., "Studies of a Gas-Filled Helical Muon Cooling Channel." Proceedings of EPAC'06, Edinburgh, p2424.
[2] Y. Derbenev and R. Johnson, "Six-Dimensional Muon Beam Cooling Using a …", Phys. Rev. STAB 8, 041002 (2005).
[3] V.S. Kashikhin et al., "Superconducting Magnet System for Muon Cooling", ASC'06, IEEE Trans. On Applied Superconductivity, 17, no. 2, p1055.
[4] V.V. Kashikhin et al., "Design Studies of Magnet Systems for Muon Cooling Channels", Proc. EPAC08, p2427.
[5] M.L. Lopes et al.,"Studies of the High-Field Solenoid Section for a Muon Helical Cooling Channel", Proc. of PAC09, p268.
[6] M.L. Lopes et al., "Studies of High-Field Sections of a Muon HCC with Coil Separation", Proc of PAC11.
[7] M.L. Lopes et al., "Magnetic Design Constraints of Helical Solenoids", WEPRI100, Submitted to IPAC'14.
[8] K. Yonehara, R.P. Johnson, M. Neubauer, Y.S. Derbenev, "A helical cooling channel system for muon colliders," MOPD076, IPAC'10.
[9] F. Marhauser et al., "RF Cavity Design Aspects for a Helical Muon Beam Cooling Channels", THPME054, Submitted to IPAC'14.
[10] F. Marhauser, private communication, 2013_07_15 HCC_Parameters.
[11] S.A. Kahn et al., THPBA26, Proc. of PAC13, p1286.